Journal of Solid State Chemistry 184 (2011) 3257–3261

Contents lists available at SciVerse ScienceDirect

Journal of Solid State Chemistry

journal homepage: www.elsevier.com/locate/jssc

Structure and resistivity of bismuth nanobelts *in situ* synthesized on silicon wafer through an ethanol-thermal method

Zheng Gao, Haiming Qin, Tao Yan, Hong Liu*, Jiyang Wang

State Key Laboratory of Crystal Materials, Bio-Micro/Nano Functional Materials Center, Shandong University, Jinan 250100, China

ARTICLE INFO

Article history:
Received 7 April 2011
Received in revised form
4 October 2011
Accepted 9 October 2011
Available online 15 October 2011

Keywords:
Bismuth nanobelts
Ethanol-thermal method
Silicon wafer
Growth mechanism

ABSTRACT

Bismuth nanobelts *in situ* grown on a silicon wafer were synthesized through an ethanol-thermal method without any capping agent. The structure of the bismuth belt–silicon composite nanostructure was characterized by scanning electron microscope, energy-dispersive X-ray spectroscopy, and high resolution transmission electron microscope. The nanobelt is a multilayered structure 100–800 nm in width and over 50 μm in length. One layer has a thickness of about 50 nm. A unique sword-like nanostructure is observed as the initial structure of the nanobelts. From these observations, a possible growth mechanism of the nanobelt is proposed. Current–voltage property measurements indicate that the resistivity of the nanobelts is slightly larger than that of the bulk bismuth material.

1. Introduction

Bismuth, a typical semimetal, has unique electric properties because of its highly anisotropic Fermi surface, low carrier concentrations, and small effective carrier mass [1,2]. Recently, bismuth nanostructures have attracted much attention because of their quantum transport and finite-size effects and potential application in magnetic field sensors, optical devices, and thermoelectric coolers or power generators [3–5]. Groups have synthesized bismuth thin films [6], nanowires [7], nanotubes [8], nanoplates [9], and nanoballs [10] through different synthesis routes. It is well known that nanobelts have different properties than nanowires and nanoparticles. Significant developments of bismuth nanostructures and a lot of essential bismuth chemistry have been made recently [11–13]. In 2005, we developed a hydrothermal method to *in situ* synthesize bismuth macro or nanoballs on the surface of silicon wafers by a hydrothermal route from bismuth hydroxide [14]. In this paper, we report an ethanol-thermal method for *in situ* synthesis of bismuth nanobelts on silicon wafers without any organic capping agent. The nanobelts grow along the surface of silicon wafer and form a novel nanostructure. This nanocomposite has potential application in electron nanodevices.

2. Experimental section

Bismuth hydroxide suspension was used as a raw material for synthesis of bismuth nanobelts on surface of silicon wafer. The reaction mechanism is based on the reaction of bismuth hydroxide and silicon at higher temperature and higher pressure [14].

Typically, synthesis of *in situ* grown bismuth nanobelts on silicon wafer comprised three steps:

(1) Cleaning the silicon wafers ((001) direction, 10 mm × 15 mm × 1 mm) sequentially using H_2SO_4/H_2O_2 [H_2SO_4 (97%)+H_2O_2 (30%)] (90 °C, 30 min), de-ionized water (ultrasonic bath 10 min, 4–6 times, to pH=7), and ethanol (ultrasonic bath 10 min).
(2) Preparing 0.01 mol/L bismuth hydroxide suspension: 0.0005 mol of analytical grade $Bi(NO_3)_3 \cdot 5H_2O$ (98%, Alfa) was dissolved in 50 ml de-ionized water to get bismuth nitric solution. Excessive ammonia hydroxide solution was dropped into bismuth nitric solution to get bismuth hydroxide precipitate. The precipitate was filtrated and washed by de-ionized water several times until pH reached 7. Then, 0.01 mol/L bismuth hydroxide suspension was prepared by dispersing all of the precipitate in de-ionized water in an ultrasonic bath for 60 min, and then adding de-ionized water to 50 ml.
(3) The hydrothermal process was performed by placing the above silicon wafer vertically into a 22 ml Teflon-lined reaction chamber. 0.5 ml of the bismuth hydroxide suspension and 18 ml of ethanol (99.5%, Sigma-Aldrich) were added into the chamber. The chamber was sealed and put into a furnace, which was preheated to 180 °C. After heating for various times, the chamber was removed and cooled down to room temperature. The silicon wafer was removed and washed with de-ionized water and then with alcohol.

Scanning electron microscopy (FE-SEM) (Field emission LEO1530 at 5–10 K), high resolution transmission electron microscope

* Correspondence to: State Key Laboratory of Crystal Materials, Shandong University, 27 Shanda Nanlu, Jinan 250100, PR China. Fax: +86 531 88362807.
E-mail address: hongliu@sdu.edu.cn (H. Liu).

0022-4596/$ - see front matter © 2011 Elsevier Inc. All rights reserved.
doi:10.1016/j.jssc.2011.10.010

(HRTEM, Hitachi HF2000) were used to characterize the morphology and microstructure of the product. Energy-dispersive X-ray spectroscopy (EDS) attached to the TEM was used to investigate the chemical composition of the as-synthesized samples.

3. Results and discussions

Fig. 1 shows SEM images of the nanobelts on silicon wafer synthesized at 180 °C for 24 h. There are some wire-like nanostructures on the surface of silicon wafer. The length of most of the wires is over 60 μm (Fig. 1a). At higher magnification, the nanowires have belt-like nanostructures (Fig. 1b). The width of the nanobelts is about 100–800 nm (Fig. 1c). Curved or curled nanobelts indicate that the thickness of the nanobelts is about 50 nm (Fig. 1d). From these observations, it is believed that one end of the nanobelts contact the silicon wafer and form a composite structure (Fig. 1e). Some nanobelts were integrated with the surface of the wafer and form a special belt-wafer structure (Fig. 1f).

The nanobelts on the surface of the silicon wafer were scraped off and dispersed in ethanol, and then dropped on a TEM grid to investigate the nanostructure. TEM and HRTEM images of the nanobelts are shown on Fig. 2. Fig. 2a shows that the nanobelts are typically 100–300 nm in width with some broad nanobelts occurring 800 nm in breadth. These results are consistent with the results from SEM observation. EDS spectrum (insert of Fig. 2a) indicates that bismuth is the main component of the sample. A small amount of silicon and oxide is present due to the amorphous silica fragments in the sample formed from the reaction between hydroxyl and silicon. The thickness of the nanobelt measured from a kinked nanobelt shown on Fig. 2b is about 40 nm. In the sample, many bismuth nanobelts are multilayered (Fig. 2c and d). The thickness of an individual layer is about 40 nm. Fig. 2e is a very broad single layered bismuth nanobelt about 500 nm in width. A typical multilayered nanobelt and its electron diffraction pattern are show in Fig. 2f and g. The diffraction pattern can be indexed to two sets of diffraction spots of rhombohedral bismuth (JCPD-80-0018). Both sets of diffraction spots are recorded along (100) crystalline plane, which demonstrates that the different layers of the nanostructure grow along the same crystal plane, {100}, and only has some dislocation between two layers. Fig. 2h and i are a single nanobelt and its diffraction pattern. The pattern can also be indexed as a diffraction pattern of (100) direction of rhombohedral bismuth structure (JCPD-80-0018), and the growth direction is along (001). The crystal structure of the nanobelts synthesized in this work is same as that of nanospheres and microballs *in situ*

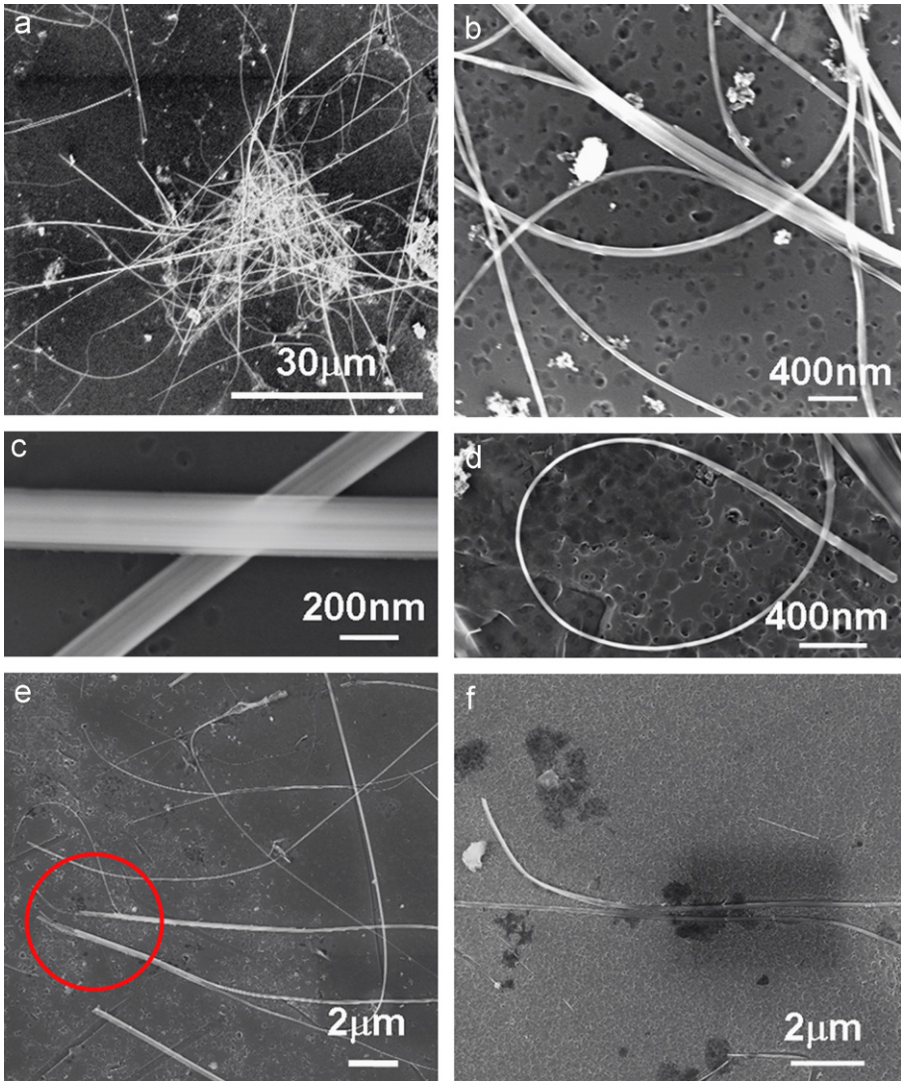

Fig. 1. SEM images of bismuth nanobelts. (a), (b) Bismuth nanobelts; (c) a bundle of bismuth nanobelts parallel to the surface of the wafer cross over a bundle of nanobelts vertical to the surface of the wafer; (d) a curved belt; the end of a belt with rectangular cross section; (e) bismuth nanobelt–silicon nanostructure, all the nanobelts started from underneath the wafer; (f) two bismuth nanobelts integrated with the silicon wafer surface.

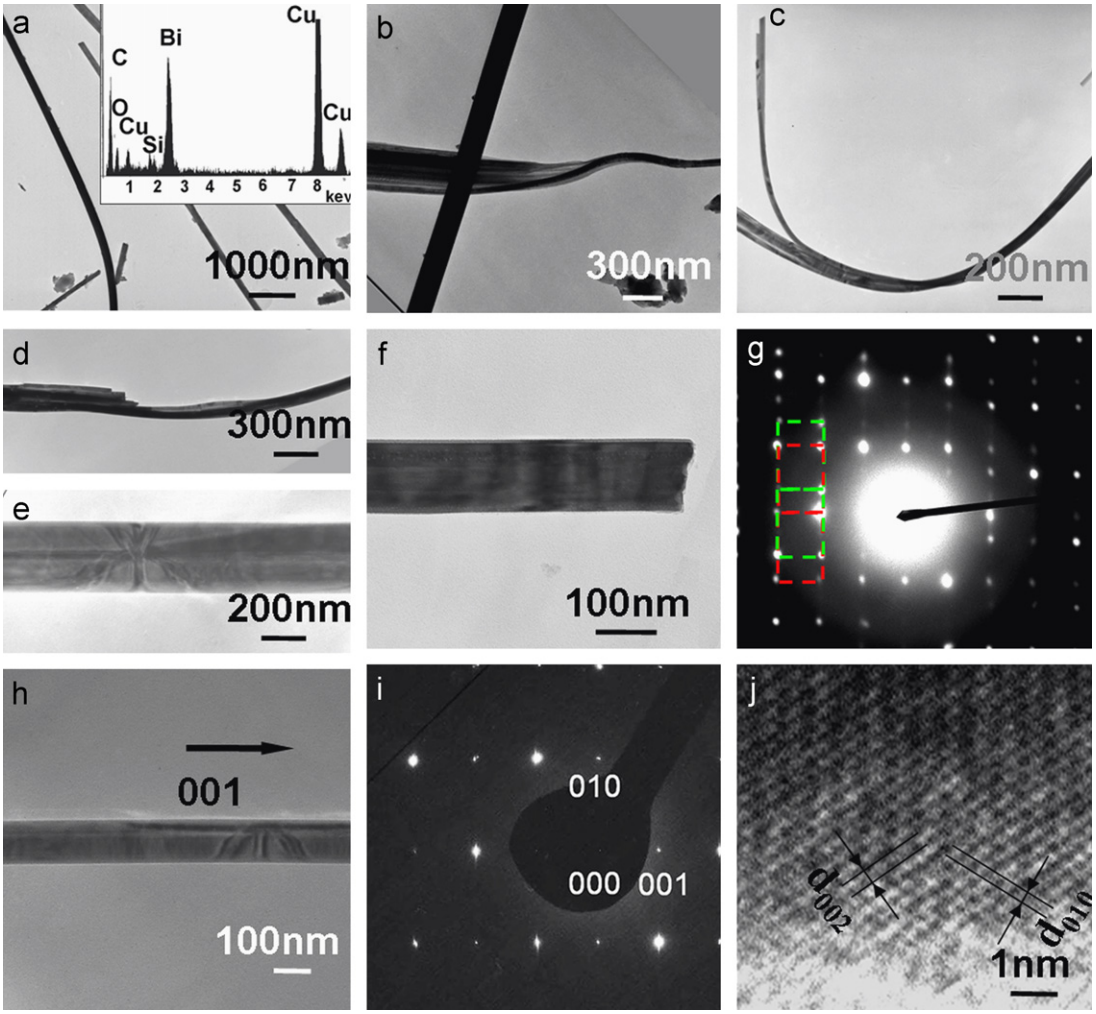

Fig. 2. TEM images, EDS, and electron diffraction pattern of bismuth nanobelts. (a) Nanobelts and their EDS (inset); (b) a straight and kinked belt; (c) a belt peeled from a multilayered nanobelt structure; (d) a bundle of the belt, the steps formed by the broken belts can be seen clearly, (e) a broad single layer nanobelt; (f) a two-layer nanobelt and (g) its electron diffraction pattern; (h) a single layer nanobelt, and (i) its electron diffraction pattern, and (j) its high resolution TEM image.

grown on silicon wafer in our previous work [14]. HRTEM image of the nanobelt shown in Fig. 2h is shown in Fig. 2j. The distance of the closest neighboring lattice spots is about 0.45 and 0.59 nm, which is consistent of d_{010} and d_{002}, and agrees with the results from electron diffraction for rhombohedral bismuth nanobelts.

The SEM images of the sample synthesized at 180 °C for 5 h give us some indication of the growth mechanism of bismuth nanobelts. Fig. 3a–c show SEM images of the nanostructures synthesized for 5 h. Some nanoballs 30–100 nm in diameter appeared on the silicon surface. At the same time, small ball-belt nanostructures, or sword-like nanostructures, can be found on the surface (Fig. 3a). SEM observation indicates that the sword-like structure is a nanobelt with a sharp edge on one end and a crown-like ball at the other end. From their width, the ball-belt nanostructures can be divided into two types: those 100 nm in width, which consistent with the nanobelts synthesized at 180 °C for 24 h, and those 30 nm in width, which correspond to the thickness of the nanobelts. These results indicate that the growth plane, (100), of some nanobelts are vertical to the wafer surface parallel to the wafer surface for others. Therefore, the nanobelts we observed on the sample synthesized at 180 °C for 24 h are suggested to grow *in situ* on the surface, not deposited from solution in the reaction chamber. Fig. 3d–g supports this conclusion. Fig. 3d is the initial part of the nanobelt that grows vertical to the surface of the silicon wafer. From this figure, we can see that the first part of the belts is buried in the wafer. The belts grow partially out of the wafer surface and then continue growing along the surface. Fig. 3g shows the part of the nanobelts whose growth plane is vertical to the silicon wafer surface. Some nanobelts also grow integrated with the surface of the wafer (Fig. 3f). This kind of nanobelt may originate from the short nanobelts shown in Fig. 3c. The ends of the nanobelts can also grow within the wafer (Fig. 3f). Some nanobelts also grow along the wafer surface, then detach and continue growing freely until they cross a nanobelt perpendicular to their growth direction. This results in the nanobelts pilling up on the surface of the wafer.

Based on the above experimental results, the mechanism of *in situ* growth of bismuth nanobelts–silicon composite is proposed. Fig. 4 illustrates the formation and growth of multilayer bismuth nanobelts on the silicon wafer. When the bismuth hydroxide–ethanol suspension is added into the reaction chamber, some bismuth hydroxide particles adhere on the surface of the wafer. When the system is heated, bismuth hydroxide reacts with silicon atoms on the surface of the wafer, and forms bismuth and silicon hydroxide

$$4Bi(OH)_3 + 3Si \rightarrow 3Si(OH)_4 + 4Bi \quad (1)$$

The bismuth atoms formed from (1) accumulate on the silicon wafer and form bismuth nuclei and then nanospheres (Fig. 4a). Because the pressure is high in this system, belt-structured bismuth

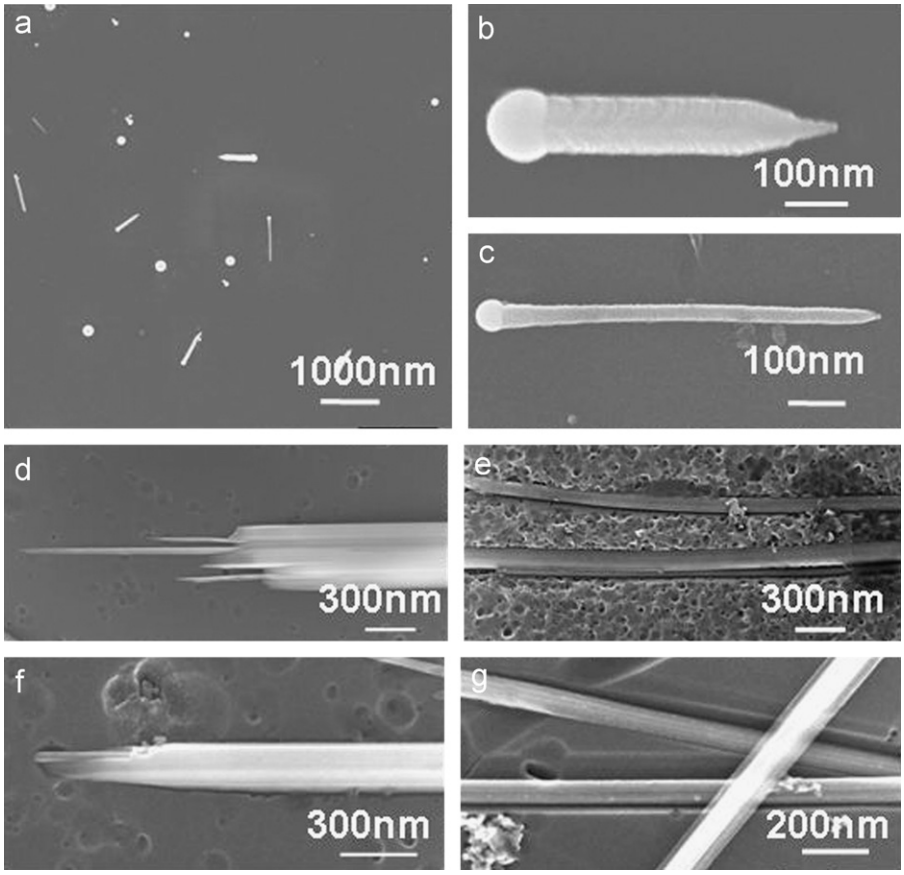

Fig. 3. Formation and *in situ* growth of bismuth nanobelts. (a) SEM image of the sample synthesized at 180 °C for 5 h; (b) a sword-like baby-nanobelt grown parallel to the surface of silicon wafer; (c) a short nanobelt grown vertical to the surface of the wafer; (d) nanobelt bundle with growth surface vertical to the silicon wafer (the ends of the belts are buried in the wafer); (e) two long nanobelts integrated with the surface of the silicon wafer; (f) multilayer nanobelt bundle with growth plane parallel to the surface of the wafer; (g) a bundle of belts passing across another bundle.

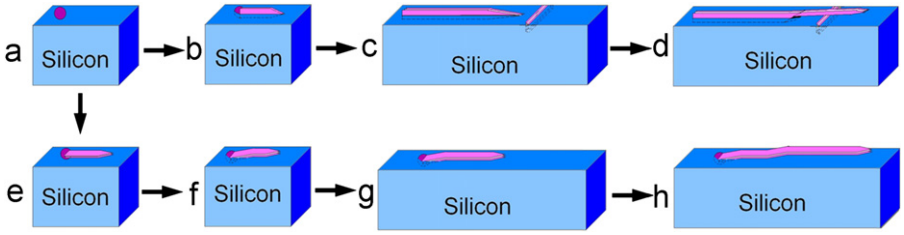

Fig. 4. Illustration of formation and growth mechanism of multilayer bismuth nanobelts. (a) The formation of bismuth spherical nucleus; (b) formation of a multilayered sword-like nanostructure; (c) the belts sink into the wafer and grow forward, meeting another bundle of belts perpendicular to the growth direction; (d) the belt kinks and grows out of the surface; (e) the nucleus forms a sword-like nanostructure parallel to the surface of the wafer; (f, g) the top of the belt sinks into the surface of the wafer and grows forward; (h) the belt finally detaches from the surface and grows freely.

nanostructures are preferentially formed, in contrast to the hydrothermal system mentioned in Ref. [14]. A single or a multilayered belt-like nanocrystal grows from the nanosphere (Fig. 4b and e). A nanosphere and a short nanobelt connect together to form the sword-like nanostructures. The growth planes of initial nanobelts grown from the bismuth sphere have two different directions: one is vertical to the surface of the silicon wafer (Fig. 4b) and the other is parallel with the surface of silicon wafer (Fig. 4f). During the growth process, the nanobelt may "dig" into the wafer and form a self-nested structure because of the "etching" effect of bismuth nanostructure on silicon wafer [14]. For the nanobelts with growth planes perpendicular to the silicon surface, parts of the nanobelts grow underneath the wafer surface. These nanobelts appear integrated with the wafer. Normally, the nanobelts can grow parallel to the surface of the wafer in a self-nest structure (Fig. 4c and d). When they meet another belt which is also integrated within the surface of the wafer, the front top the belt will kink and continue to grow out of the wafer. For the nanobelts with growth planes parallel to the surface of the wafer (shown in Fig. 4f), the initial section of the belt can "dig" into the wafer (Fig. 4g) and subsequent sections of the belt grow out of the wafer. The large surface area of the parallel growth nanobelt may hinder the "digging" of the nanobelts (Fig. 4g and h), which means that when the reaction occurs over longer times nanobelts accumulate on the surface of the wafer.

To investigate the electrical properties of the nanobelts, a three-layer bismuth nanobelt about 800 nm in breadth, 250 nm in thickness, and 8800 nm in length was used to measure *I–V* characteristics. The nanobelt was aligned on a pair of gold electrodes. A layer of gold was coated on the contact ends of the nanobelt by focus ion beam (FIB) to lower the contact resistance between the electrodes and the nanobelt. An *I–V* curve of this belt is shown in Fig. 5. The measured electric resistance of this nanobelt is $2 \times 10^4\ \Omega$. Calculated

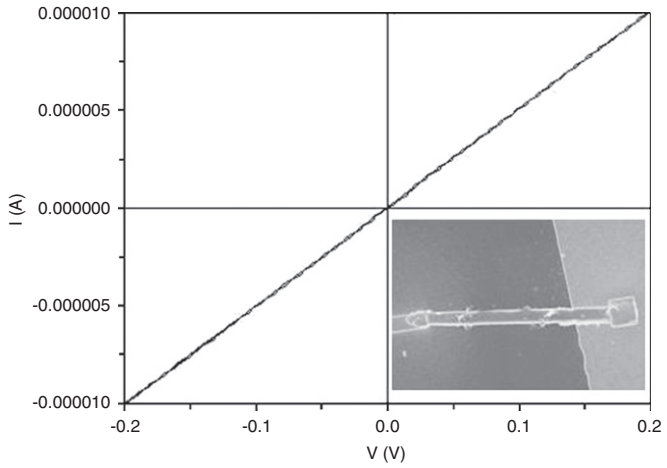

Fig. 5. *I–V* curve measured on a nanobelt bundle (inset).

resistivity of the nanobelt is $0.27 \times 10^{-3}\,\Omega$ m, which is larger than that of bulk bismuth material, $0.12 \times 10^{-3}\,\Omega$ m. The increase of the resistivity of the nanobelts is most likely caused by the enormous dangling bonds on the belt surface. Wider nanobelts would provide bigger cross sectional area which would reduce the resistivity of the nanobelts.

4. Conclusions

Bismuth nanobelts *in situ* grown on silicon wafer were synthesized through an ethanol-thermal method by using bismuth hydroxide as a raw material at 180 °C for 24 h. The nanobelts are typically multilayered structures 100–800 nm in width, 50 nm in thickness, and over 30 μm in length. A special sword-like nanostructure was found in the sample synthesized at 180 °C for 5 h. This structure is thought to be the initial structure of the nanobelt. The nanobelts integrate on the surface of the silicon wafer and form a special bismuth–silicon nanostructure, which has a potential application for some nanodevices. The *I–V* properties of an individual multilayered nanobelt were measured and found to have different properties that bulk bismuth materials. Because bismuth is a semimetal with unique physical properties, bismuth nanobelts may find application in sensitive magnetic sensors or used to build other electronic devices.

Acknowledgment

This research was supported by NSFC (NSFDYS: 50925205, Grant: 50990303, 50872070, IRG: 50721002), Independent Innovation Foundation of Shandong University, (2009JC011) and the Program of Introducing Talents of Discipline to Universities in China (111 program no. b06015).

References

[1] F.Y. Yang, K. Liu, K. Hong, D.H. Reich, P.C. Searson, C.L. Chien, Science 284 (1999) 1335.
[2] Y.F. Komnik, E.I. Bukhshtab, Y.V. Nikitin, V.V. Andrievskii, Zh. Eksp. Teor. Fiz. 60 (1971) 669.
[3] Z. Zhang, X. Sun, M.S. Dresselhaus, J. Ying, Appl. Phys. Lett. 73 (1998) 1589.
[4] J. Heremans, C.M. Thrush, Y.-M. Lin, S. Cronin, Z. Zhang, M.S. Dresselhaus, J.F. Mansfield, Phys. Rev. B 61 (2000) 2921.
[5] Z. Zhang, X. Sun, M.S. Dresselhaus, J.Y. Ying, J. Heremans, Phys. Rev. B 61 (2000) 4850.
[6] D.W. Song, W.-N. Shen, B. Dunn, C.D. Moore, M.S. Goorsky, T. Radetic, R. Gronsky, G. Chenb, Appl. Phys. Lett. 84 (2004) 1883.
[7] Y. Hasegawa, Y. Ishikawa, T. Komine, T.E. Huber, A. Suzuki, H. Morita, H. Shirai, Appl. Phys. Lett. 85 (2004) 917.
[8] B. Yang, C. Li, H. Hu, X. Yang, Q. Li, Y. Qian, Eur. J. Inorg. Chem., 2003 () 3699.
[9] R. Fu, S. Xu, Y. Lu, J. Zhu, Cryst. Growth Des. 5 (4) (2005) 1379.
[10] J. Wang, X. Wang, Q. Peng, Y. Li, Inorg. Chem. 43 (2004) 7553.
[11] P.S. Berdonosov, V.A. Dolgikh, P. Lightfoot, J. Solid. State. Chem. 180 (2007) 1533.
[12] Hong Deng, Junwei Wang, Qing Peng, Xun Wang, Yadong Li, Chem. Eur. J. 11 (2005) 6519.
[13] Laura López-de-la-Torre, Alexandra Friedrich, J. Solid State Chem. 182 (2009) 767.
[14] H. Liu, Z.L. Wang, J. Am. Chem. Soc. 127 (2005) 15322.